

High-contrast all-optical bistable switching in photonic crystal microcavities

Mehmet Fatih Yanik and Shanhui Fan^{a)}

Ginzton Laboratory, Stanford University, Stanford, California 94305

Marin Soljačić

Department of Physics, Massachusetts Institute of Technology, Cambridge, Massachusetts 02139

(Received 2 June 2003; accepted 6 August 2003)

We present a bistable photonic crystal configuration consisting of a waveguide sided coupled to a single-mode cavity with instantaneous Kerr nonlinearity. We show that such a configuration can generate extremely high contrast between the bistable states in its transmission with low input power. We also provide an analytic theory that can completely account for the entire transient switching dynamics, as revealed by finite difference time domain simulations. © 2003 American Institute of Physics. [DOI: 10.1063/1.1615835]

Optical bistable devices are of great importance for all-optical information processing applications.¹ Recently, it was shown that optical bistability could be achieved in a nonlinear photonic crystal (PC).^{2–5} The use of a PC resonator results in greatly reduced power requirements. For practical applications of integrated two-port bistable devices, however, an important consideration is the contrast ratio in the transmission between the two bistable states. A high contrast ratio is beneficial for maximum immunity to noise and detection error, and for fan-out considerations.

In this letter, we present an alternative PC configuration with a greatly improved contrast ratio in its transmission. We also provide an analytic theory that can account for the switching dynamics in nonlinear PC structures. Unlike previously considered two-port PC devices based upon direct-coupled resonator geometry [Fig. 1(a)],^{2–4} our proposed configuration consists of a waveguide side-coupled to a single-mode cavity with Kerr nonlinearity [Fig. 1(b)]. Similar to the direct-coupled resonator geometry, the optical energy inside the cavity can exhibit bistable dependence on the incident power level, and can switch between two states with either low or high optical energy. In general, due to weakness of nonlinearity, it is necessary to choose the operating frequency to be in the vicinity of the resonant frequency in order to reduce the incident power requirement. Doing so, however, also decreases the ratio of the optical energy of the two states inside the resonator.

In the direct-coupled resonator geometry as shown in Fig. 1(a), the transmitted power is proportional to the optical energy inside the cavity. Thus, the contrast ratio in the transmitted power becomes limited. In comparison, for the side-coupled geometry [Fig. 1(b)], one could take advantage of the interference between the propagating wave inside the waveguide and the decaying wave from the cavity, to greatly enhance achievable contrast ratio in the transmission between the two bistable states.

Using a similar procedure to that outlined in Ref. 4, the transmitted power ratio T for a nonlinear side-coupled resonator can be analytically written as

$$T \equiv \frac{P_{\text{trans}}}{P_{\text{in}}} = \frac{(P_{\text{ref}}/P_0 - \delta)^2}{1 + (P_{\text{ref}}/P_0 - \delta)^2}, \quad (1)$$

where P_{in} , P_{ref} , and P_{trans} are, respectively, the input, reflected, and transmitted powers such that $P_{\text{in}} = P_{\text{trans}} + P_{\text{ref}}$. $P_0 = 1/[\kappa Q^2 \omega_{\text{res}} n_2(r)|_{\text{max}}/c]$ is the characteristic power of the cavity and κ is the dimensionless scale invariant nonlinear feedback parameter proportional to the overlap of the cavity mode with the nonlinear region.⁴ $\delta = (\omega_{\text{res}} - \omega_0)/\gamma$ is the detuning of the incident excitation frequency ω_0 from the cavity resonance frequency ω_{res} , and the cavity decay rate γ is related to the cavity quality factor Q by $\gamma = \omega_{\text{res}}/(2 \cdot Q)$. $n_2(r)$ and c are, respectively, the spatially varying Kerr coefficient, and the speed of the light. For a particular set of parameters to be detailed later, the behavior of P_{trans} as a function of P_{in} is shown as the red solid line in Fig. 2. Although the material response is instantaneous, this device displays memory effects such that its current state depends not only on the current input, but also on the past state of the system, yielding the hysteretic trajectories shown in Fig. 2. We note that one of the bistable states can possess a near-zero transmission coefficient, and thus the contrast ratio can be infinitely high. This occurs when there is sufficient energy inside the cavity such that the resonance frequency of the cavity coincides with that of the incident field.

As a physical implementation of the theoretical idea just presented, we consider the PC structure shown in the inset of Fig. 2. The crystal consists of a square lattice of high dielectric rods ($n=3.5$) with a radius of $0.2a$, (a is the lattice constant) embedded in air ($n=1$). We introduce the waveguide into the crystal by removing a line of rods, and create

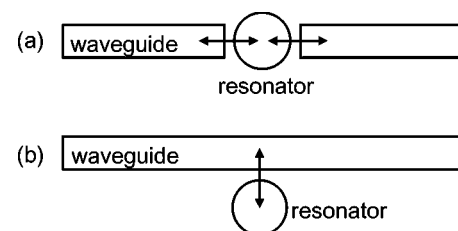


FIG. 1. Schematic configuration for (a) a waveguide directly coupled to a cavity and (b) a waveguide side-coupled to a cavity.

^{a)}Electronic mail: shanhui@stanford.edu

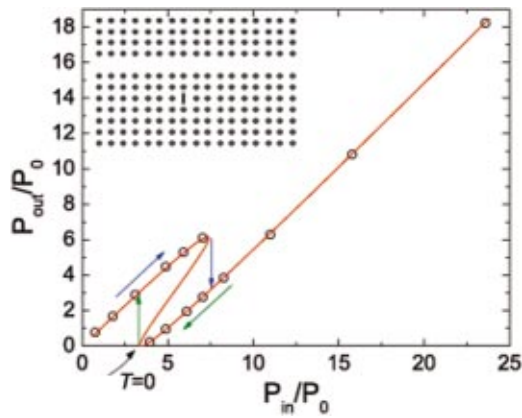


FIG. 2. (Color) Input versus output power for the side-coupled PC cavity structure shown in the inset. Open circles are results from FDTD simulations, and the solid line is calculated using Eq. (1). Blue and green arrows show the hysteresis loop.

a side-coupled cavity that supports a single resonant state by introducing a point defect with an elliptical dielectric rod, with the long and short axis lengths of a and $0.2a$, respectively. The defect region possesses instantaneous nonlinear Kerr response with a Kerr coefficient of $n_2 = 1.5 \times 10^{-17} \text{ W/m}^2$, which is achievable using nearly instantaneous nonlinearity in many semiconductors.⁶ The use of the elliptical rod generates a single-mode cavity and also enhances the field localization in the nonlinear region.

We perform nonlinear finite difference time domain (FDTD) simulations⁷ for the TM case with electric field parallel to the rod axis for this PC system. The simulations use 12×12 grid points per unit cell, and incorporate a perfectly matched layer boundary condition specifically designed for PC waveguide simulations.⁸ At a low incident power level at which the structure behaves linearly, we determine that the cavity has a resonant frequency of $\omega_{\text{res}} = 0.371(2\pi c/a)$, which falls within the band gap of the PC, a quality factor of $Q = 4494$, and a nonlinear feedback parameter $\kappa = 0.185$. Using these parameters, the theory predicts a characteristic power level of $P_0 = 4.4 \text{ mW}/\mu\text{m}$ for the $1.55\text{-}\mu\text{m}$ wavelength used in our simulations. For a three-dimensional structure, with the optical mode confined in the third dimension to a width about half a wavelength, the characteristic power is only on the order of a few milliwatts.

To study the nonlinear switching behavior, we excite an incident cw in the waveguide detuned by $\delta = 2\sqrt{3}$ from the cavity resonance ($\delta = \sqrt{3}$ is the minimum detuning requirement for the presence of bistability). We vary the input power and measure the output power at steady state, as shown by the open circles in Fig. 2. In particular, we observe a bistable region between $3.39P_0$ and $7.40P_0$. The FDTD results fit almost perfectly with the theoretical prediction, generated using Eq. (1) and exhibited as a solid line in Fig. 2. Note that on the theory curve, the region where there are no FDTD data points is unstable. The contrast ratio between the upper and lower branch approaches infinity as transmission drops to zero in the lower branch in transmission.

Figure 3 shows the field patterns for the two bistable states for the same input cw power level of $3.95P_0$. Figure 3(a) corresponds to the high transmission state. In this state, the cavity is off-resonance with the excitation. The field in-

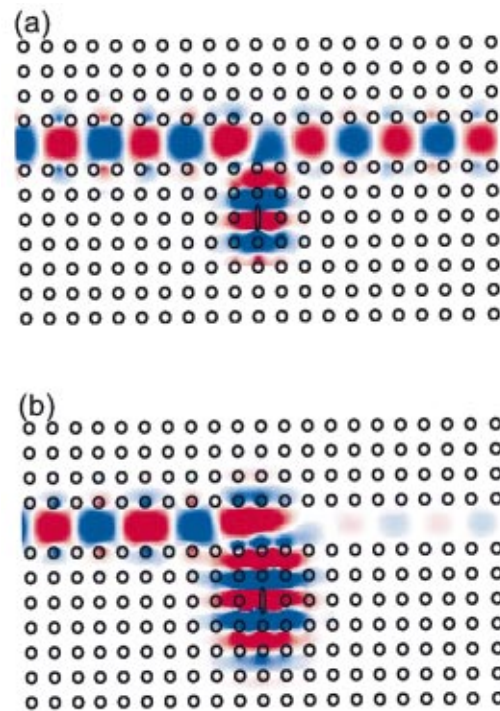


FIG. 3. (Color) Electric field distributions in the PC structure for (a) the high transmission state and (b) the low transmission state. The input power is $3.95P_0$ for both cases. Red and blue represent large positive or negative electric fields, respectively. The same color scale is used for both panels. The black circles indicate the positions of the dielectric rods in the PC.

side the cavity is low, and thus the decaying field amplitude from the cavity is negligible. Figure 3(b) corresponds to the low transmission state. Here, the field intensity inside the cavity is much higher, pulling the cavity resonance frequency down to the excitation frequency of the incident field. The decaying field amplitude from the cavity is significant, and it interferes destructively with the incoming field. Thus, it is indeed the interference between the wave propagating in the waveguide and the decaying amplitude from the cavity that result in the high contrast ratio in transmission.

The FDTD analysis also reveals that the transmission can be switched to the lower branch from the upper branch with a pulse. Figure 4 shows the peak power in each optical period in the waveguide as a function of time, as we switch

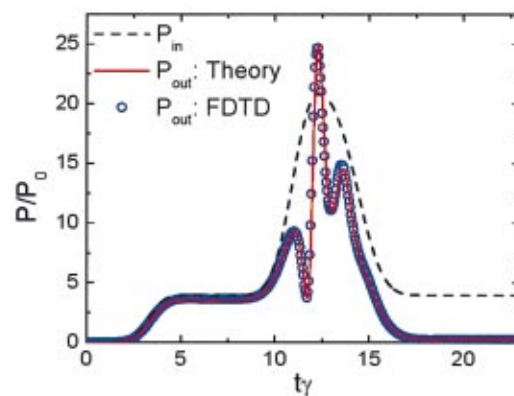


FIG. 4. (Color) The black curve represents the input power as a function of time. The red curve and the blue open circles show the output power levels, calculated respectively by the CM theory [Eq. (2)], and by FDTD simulations.

the system between the two bistable states shown in Fig. 3. As the input is initially increased to the cw power level of $3.95P_0$, the system evolves into a high transmission state, with the transmitted power of $3.65P_0$. The switching then occurs after a pulse, which possesses a peak power $20.85P_0$, the same carrier frequency as that of cw, and a rise time and a width equal to the cavity lifetime, is superimposed upon the cw excitation. The pulse pushes the stored optical energy inside the cavity above the bistable threshold. After the pulse has passed through the cavity, the system switches to the bistable state with low transmission power of $0.25P_0$.

The switching dynamics, as revealed by the FDTD analysis, can in fact be completely accounted for with temporal coupled-mode (CM) theory. The CM equations⁹ relating the input, reflected, and transmitted power can be expressed in the following form for the side-coupled cavity structure:

$$\frac{dS_{\text{ref}}}{dt} = i\omega_{\text{res}} \left(1 - \frac{1}{2Q} \frac{|S_{\text{ref}}|^2}{P_0} \right) S_{\text{ref}} - \gamma S_{\text{ref}} - \gamma S_{\text{in}}, \quad (2)$$

where S_{in} and S_{ref} are proportional to the incident and reflected field amplitudes, respectively, such that $P_{\text{in}} = |S_{\text{in}}|^2$, $P_{\text{ref}} = |S_{\text{ref}}|^2$, and $P_{\text{out}} = P_{\text{in}} - P_{\text{ref}}$. It is important to note that the FDTD analysis takes into account the full effects of the nonlinearity. The CM theory, on the other hand, neglects higher harmonics of the carrier frequency generated by the nonlinearity. Nevertheless, since the switching and the cavity

decay time scales are far larger than the optical period, the agreements between the CM theory and FDTD simulations are excellent as shown in Fig. 4. Thus, we show that the nonlinear dynamics in PC structures can be completely accounted for using CM theory, which provides a rigorous and convenient framework for analyzing complex nonlinear processes and devices.

The simulations were performed at the Pittsburgh Supercomputing Center (PSC), and at the Center for Advanced Computation (CAC) at University of Michigan, with the support of a NSF-NRAC grant. One of the authors (M.F.Y.) gratefully acknowledges support of Stanford Graduate Fellowship.

¹H. M. Gibbs, *Optical Bistability: Controlling Light with Light* (Academic, Orlando, FL, 1985).

²E. Centeno and D. Felbacq, Phys. Rev. B **62**, R7683 (2000).

³S. F. Mingaleev and Y. S. Kivshar, J. Opt. Soc. Am. B **19**, 2241 (2002).

⁴M. Soljacic, M. Ibanescu, S. G. Johnson, Y. Fink, and J. D. Joannopoulos, Phys. Rev. E **66**, 055601(R) (2002).

⁵M. Soljacic, C. Luo, J. D. Joannopoulos, and S. Fan, Opt. Lett. **28**, 637 (2003).

⁶M. Sheik-Bahae, D. C. Hutchings, D. J. Hagan, and E. W. Van Stryland, IEEE J. Quantum Electron. **27**, 1296 (1991).

⁷A. Taflov and S. C. Hagness, *Computational Electrodynamics* (Artech House, Norwood, MA, 2000).

⁸M. Koshiba and Y. Tsuji, IEEE Microwave and Wireless Comp. Lett. **11**, 152 (2001).

⁹H. A. Haus, *Waves and Fields in Optoelectronics* (Prentice-Hall, New Jersey, 1984).